Seismic Behavior of the Partially Prefabricated Laminated RC Walls Under Different Axial Ratios

H. M. Zhang
State Key Laboratory of Disaster Reduction in Civil Engineering, Tongji University, Shanghai, China

X. L. Lu
State Key Laboratory of Disaster Reduction in Civil Engineering, Tongji University, Shanghai, China

J. B. Li
State Key Laboratory of Disaster Reduction in Civil Engineering, Tongji University, Shanghai, China

SUMMARY:
The partially prefabricated laminated (RC) walls mentioned is this kind of seismic prevention element with part prefabricated concrete plate and cast in place concrete plate. 4 typical laminated walls without openings, 4 laminated walls with openings, and 1 common cast-in-place RC walls were tested under cyclic test. The seismic behaviour were analysed by the finite element software based on the test results and simulated results. The laminated walls and the common cast-in-place wall under different axial forces were simulated also. Seismic behaviour analysis indicates that the laminated walls are vulnerable to failure under high axial force compared with the cast-in-place walls, so the laminated walls are not suggested to apply in the bottom stories of the high-rise structures especially in areas vulnerable to earthquake.

Keywords: Laminated wall, RC wall, low-cyclic reversed test, experimental study, numerical simulation

1. GENERAL INSTRUCTIONS

It is well known that the reinforced concrete (RC) shear wall can provides both vertical and horizontal load carrying capacity. So it has been widely used in high-rise buildings. The prefabricated RC wall structure has attracted extensive attentions worldwide for the advantages of prefabrication technologies in construction. But the seismic behaviour of the prefabricated RC walls still remains vague.

In the light of the research and application, prefabricated shear walls are mostly used as non-bearing element. While recently, a type of partially prefabricated and partially cast-in-place laminated RC shear wall has been applied in pilot projects in Japan and China. The prefabricated part of this kind of RC shear wall is constructed with horizontal and vertical steel bars (Saito et al. 1995), and the embedded columns can also be set as the requirement. The cast-in-place part of the laminated wall is constructed with concrete and reinforcement as the common cast-in-place RC wall.

In order to investigate the seismic behaviours of this partially prefabricated laminated wall, experimental work subjected to low-cyclic reversed loads and nonlinear finite element analysis under different axial forces were conducted. The seismic behaviour of the laminated walls will be addressed in this paper.

2. REVERSED CYCLICAL LOAD TEST

2.1. The Tested Specimen

The experimental study was conducted in the State Key Laboratory of Disaster Reduction in Civil

Engineering in Tongji University. Three kinds of specimens were designed. Strengthening bars were set across the top and bottom beams and the walls as HRB400Φ10@150. Foe embedded columns located at the edges of the RC walls had been verified to have influence on the load carrying capacity and deformation property (Zhang et al. 2007). The embedded columns and longitudinal bars were set in specimen SWA and the cast-in-place parts of PCFA and PCFB (Ministry of Construction of the People's Republic of China 2010) in this study. The dimension, reinforcement and axial force details of the tested specimens are listed in Table 1.

Table 1. Details of the tested specimens

Specimen number	Embedded column parameters			Distributing bars （HRB400）		Axial force(kN)	Axial ratio
	Dimension (mm)	Longitudinal bars (HRB335)	Stirrup bars (HRB400)	horizontal	vertical		
PCFA1~4	180×400	6Φ14	Φ 8@150	Φ 8@150		1200	0.2
PCFB1~4	180×400	6Φ14	Φ 8@150	Φ 8@150		600	0.1
SWA	250×400	6Φ14	Φ 8@150	Φ 8@150		1200	0.2

Note: the dimension of the specimen is 1800mm×1500mm×250mm

Horizontal and vertical trusses were set across the prefabricated and the cast-in-place parts to enhance the interfacial bonding capacity of the laminated specimens. A layout of the internal trusses is shown in Figures 1 (a) and (b). Each steel truss was constructed by the upper and lower steel bars and they were connected by the web bars. The lower bars of the steel truss were connected to the reinforcement bars of the prefabricated part and were cast into the concrete plate. During the onsite construction, the prefabricated plate was fixed into the bottom beam by bolts and steel angles, which will be taken off after the cast-in-place part is constructed, as shown in Figure 1 (c).

In general, the prefabricated part is firstly manufactured in factory, and then the prefabricated part is transport to site and used as part of the module boards for the cast-in-place part. The support elements are taken off after the cast-in-place concrete reaches its design strength. Therefore, the concrete of the two parts of the laminated walls has different ages, and that may cause the incompatibility of the laminated walls.

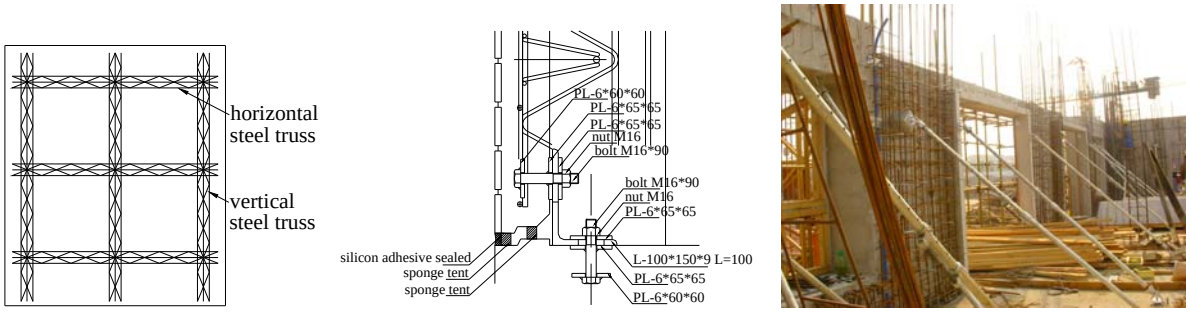

(a) (b) (c)

Figure 1. Construction details (unit: mm)—(a) steel trusses of the prefabricated part; (b) construction diagram of the laminated wall; (c) on site picture of the laminated walls

Figure 2 shows the connection details between the test specimens and the top and bottom support beams. The vertical distribution bars and the longitudinal bars of embedded columns in the specimens are stuck into the top and bottom beams. Strengthening reinforcement bars are also set between the specimens and the top/bottom beams to insure effective connection between them.

The axial load is applied by jacks. The top support beam has a section of 400mm × 400mm. The rigidity of the top support beam in the vertical direction is large enough to transfer the axial force to the specimens without noticeable deformation of the support beam itself. The bottom beam is fixed in the platform of the laboratory by enough bolts to insure the connection strength.

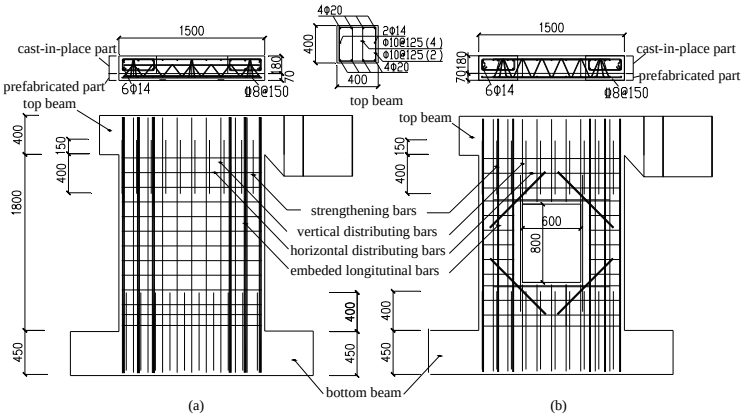

Figure 2. Details of the specimen (unit: mm) — (a) PCFA; (b) PCFB

2.2. The Tested Material Properties

The details of the tested material properties including the concrete and the steel are listed in Tables 2 and 3.

Table 2. Material properties of concrete

Specimen number	f_c / MPa	f_{cu} /MPa	E_c / N m^{-2}
PCFA1~4	27.7	23.8	3.35×10^{10}
PCFB1~4	33.6	27.8	3.66×10^{10}
SWA	27.7	19.7	2.90×10^{10}
Prefabricated concrete	34.0	26.0	3.00×10^{10}

f_c —concrete cube pressure strength; f_{cu} —concrete axis pressure strength, E_c —concrete elastic modulus

Table 3. Material properties of Steel

Steel bar type	Diameter	f_y / MPa	f_u / MPa	E_s / N mm^{-2}	ε_y / $\mu\varepsilon$
Φ14	14mm	372.80	546.93	2.0×10^5	1864
Φ12	12mm	371.67	535.2	2.0×10^5	1849
Φ10	10mm	380.24	604.5	2.0×10^5	1901
Φ8	8mm	385.03	617.04	2.0×10^5	1925

f_y —yield tension strength; f_u —ultimate tension strength; E_s —steel bar elastic modulus; ε_y —yield strain

2.3. Test Loading Process

The axial pressure was applied by jacks seated on the top of the wall with the vertical force of 1200 kN for the solid laminated walls without openings (PCFA), and 600 kN for the laminated walls with an opening (PCFB). The horizontal load was applied by the electro-hydraulic servo loading device.

All the specimens were loaded by constant vertical pressure and reversed cyclic lateral (horizontal in-plane) load (Salonikios et al. 1999). The lateral load was applied by displacement-controlled loading method. The predefined vertical load was set to 1200 kN (for specimen PCFA) or 600 kN (for specimen PCFB) before the lateral load was applied, and was maintained to the constant value during the whole test procedure.

Each step interval of the lateral displacement was set to 1 mm and each loading stage was maintained for one cycle at the early stage of the loading procedure. The displacement step interval was increased to 2 mm after the specimen was yield and each loading stage was maintained for three cycles. The specimen was declared failed when the lateral force decreased to 85% of the maximum lateral force value or the specimen was obviously damaged before reaching the normal ultimate point. The failure

pictures are shown in Figure 3.

(a) (b) (c) (d)

Figure 3. failure picture - (a) front view of PCFA; (b) side view of PCFA; (a) front view of PCFB; (b) side view of PCFB

3. NUMERICAL SIMULATION STUDY

The static nonlinear analysis method (pushover method) is adopted in this numerical simulation in light of the loading conditions of the real experiment using the finite element analysis software-ABAQUS.

The finite element model was developed in accordance to the experimental model considering the bonding property of the interfaces between prefabricated part and cast-in-place part. And the material parameters adopted in the numerical simulation were determined according to the experimental material properties.

In this simulation program, the laminated shear walls were constructed by concrete, boundary longitudinal bars, distribution bars and interface spring elements (Li and Li 2006). Concrete Damaged Plasticity Model (Huan et al. 2008) and Kent-Park constitutive relationship model (Kent et al. 1971) were applied to simulate the confined concrete (Zhang et al. 2010a,b). The compression value of the concrete in the simulation program was defined by the actual tested concrete material value as listed in Table 2. The piecewise linear relationship was applied in the plastic constitutive relationship of the longitudinal steel bars and distributing steel bars.

The bottom of the specimen was totally constrained and the vertical pressure was uniformly distributed on the top. The lateral load was applied on the nodes of the top section and controlled by displacement. The old and new concrete parts were constructed by two plates of solid elements, which were interconnected by three-dimensional springs as shown in Figure 4. Besides, the steel bar elements were designed as solid model and located in the constrained area of the cast-in-place part. The scattering bars were regarded to scatter in the concrete uniformly.

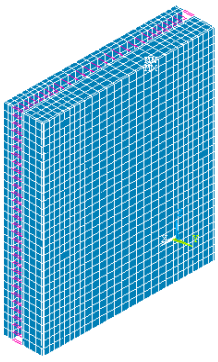

Figure 4. Finite element model

4. DISCUSSION OF EXPERIMENT AND SIMULATION RESULTS

In general, the experimental lateral force-top drift hysteretic skeleton curves of the rectangular shear walls agree with the monotonous pushover test results (Dong et al. 2007). Therefore, pushover analysis method was adopted to investigate the seismic behaviour of the walls to avoid convergence problem in cyclic hysteretic analysis. The experimental scenarios were first simulated through the

pushover analysis program, and the simulation result was verified by the experimental results. The structural properties of the laminated walls under different axial ratios and the interface integrity of the laminated walls were investigated. Since the behaviour of this laminated wall under high axial force is a key point, specimens were analysed under different axial ratios from 0.1 to 0.5.

4.1. Seismic Behaviour of the Tested Specimens

The axial ratio of the shear wall in the middle height buildings is often within 0.1 to 0.3, so the axial ratio of the cyclic test of the solid specimen was defined as 0.2, and the axial ratio of the specimen with an opening is 0.1 as the typical axial ratio. The simulation analysis of the test specimens was executed according to the real test loading conditions.

The tested specimens experienced from elastic stage to plastic stage when the top lateral displacement reached 4 mm to 8 mm through the whole loading procedure. Short horizontal and inclined cracks appeared at the corner of the cast-in-place part at first, and then extended to the lower corner of the prefabricated part for the laminated specimens. With the increase of the loading, the cracks developed in length and width, and the rigidity decreased. If the lateral load on the top beam decreased to about 85% of the maximum value at the later stage of the test and the concrete at the lower corner of the specimen crushed, the test was terminated, with the ultimate displacement amplitude of 30 mm to 46 mm.

The vertical pressure exerted on the specimens was similar with the real experiments, while the lateral load of the simulation program was monotonous loads. Therefore, the simulated result is not symmetric as the tested one, but that still can provide meaningful structural behaviour information. The maximum stress is at the compression corner. And the main damage at the foot corner is also controlled the failure of the specimen. Both the tested results and the simulated results indicate that the vulnerable part is at the foot corner of the walls.

Both the simulated results and the tested results show that the maximum stress occurs at the foot corner of the specimen. The corners of the opening are also vulnerable to damage due to the cross-section variation, which is consistent with the related research (Hallinan and Guan, 2007). In general the damage pattern of the solid laminated walls is similar to the common cast-in-place RC wall. They are all failed at the foot corner, and with the similar cracks distribution. In this test and simulation program, there was no obvious damage at the new and old concrete interface under the experiment loading condition.

The lateral force-deformation curves of the 4 solid laminated specimens PCFA1 to PCFA4 and 1 cast-in-place specimen (tested: SWA, PCFA; simulated: SWAC, PCFAC) are shown in Figure 5(a). The simulated curve of PCFAC agrees with the tested curves PCFA1~4 generally, especially on the ultimate strength. Comparing the solid laminated specimens with the cast-in-place specimen, no apparent difference on the damage pattern and lateral load-top drift relationship was found. Figure 5(b) shows the lateral force and top drift curves of PCFB1~BCFB4 (tested) and PCFBC (simulated) for the laminated specimens with an opening. This group of curves also indicate that the simulated result agrees to the tested results at the early stage of loading procedure. We still found that the simulated curve is lower than the tested value, which is possibly due to the strengthening steel bars around the opening and between the walls and the top and bottom beams in real test, whose effect is ignored in the simulation analysis. But the simulation result is acceptable in general, especially at the early stage of the loading process.

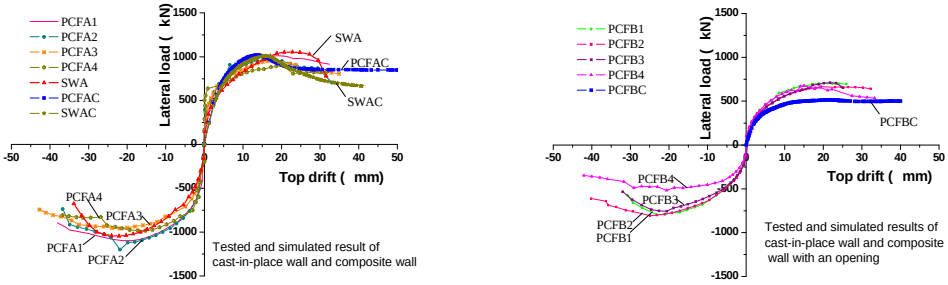

(a) (b)

Figure 5. Tested and simulated force-deformation curves of the cast-in-place wall and laminated walls without openings; (a) PCFA; (b) PCFB

4.2. Simulation under Different Axial Ratios

To clarify whether the interface of the new and old concrete has enough strength to insure the integrity of the laminated wall under high axial pressures, the simulation program is designed under different axial ratios.

The axial ratio is defined as the ratio of axial forces over the sectional ultimate capacity of axial compressive forces. During the simulation analysis, the horizontal load was exerted on the nodes of the top cross-section which were coupled together with the same displacement on X direction. In addition, the entire node was constrained on Y direction to confirm there was no out-of-plane displacement. The bottom nodes were totally restrained in each degree of freedom according to the test condition. The simulation results of the lateral load-top drift curves under different axial ratios are shown in Figures 6, including the cast-in-place RC wall, solid laminated wall without openings and the laminated wall with an opening respectively.

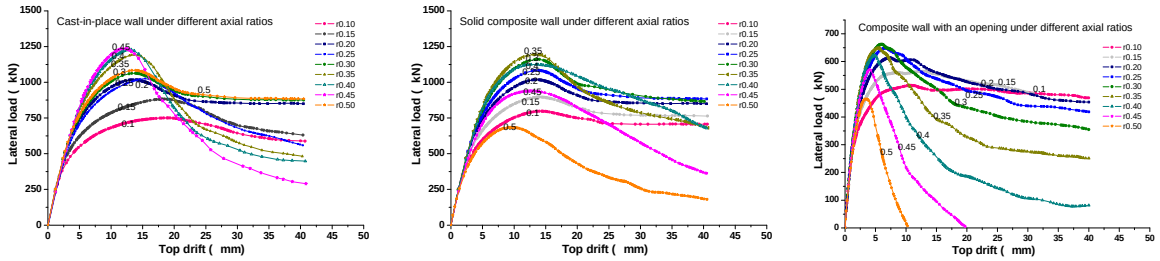

(a) (b) (c)

Figure 6. Simulated force-deformation curves under different axial ratios; (a) the cast-in-place wall; (b) the solid laminated wall without openings; (c) the laminated wall with an opening

The cast-in-place wall under different axial ratios was firstly investigated as demonstrated in Figure 6. The lateral load carrying capacity increases as the axial ratio increases until the axial ratio reaches 0.45. The lateral load carrying capacity decreases after the axial ratio is beyond 0.45. The increase ratio of the load carrying capacity of the cast-in-place wall becomes smaller before the axial ratio is less than 0.45 and the load carrying capacity decreases dramatically when the axial ratio is larger than 0.45, as shown in Figure 6 (a) and Figure 7 (a).

The behaviour of the laminated specimens under different axial ratios is shown in Figure 7(b). The lateral load carrying capacity of the solid laminated wall increases with the increase of the axial ratio before the axial ratio reaches 0.35, but the increasing amplitude becomes smaller than before. And the lateral load carrying capacity decreases dramatically when the axial ratio increases beyond 0.35, which may induce sudden failure of an element or a structure, as shown in Figure 6 (a) and Figure 7 (a). The development pattern of load carrying capacity of the solid laminated wall is similar to the cast-in-place wall, but the turning point of the axial ratio for the maximum lateral carrying capacity is different,

which is 0.35 for the solid laminated specimen and 0.45 for the cast-in-place specimen in this study. That indicate the laminated walls are more sensitive to the axial ratio. Increasing the axial ratio to a critical value will lead to the change of the pattern of the force-top drift, and the lateral load carrying capacity will reach a peak value under this critical value. And this critical value of laminated walls is less than that of the common cast-in-place walls.

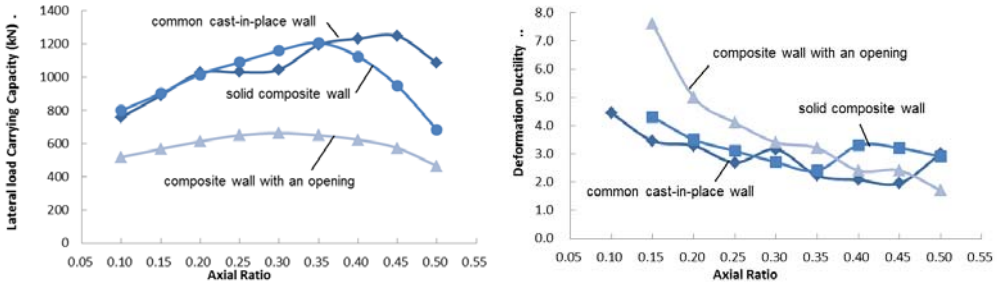

(a) (b)

Figure 7. Lateral load carrying capacity and displacement ductility of the walls under different axial ratios—(a) Lateral load carrying capacity; (b) Deformation ductility

The axial ratio of the laminated wall with an opening is defined as the ratio of axial force over the ultimate compressive force capacity of the cross-section above or below the opening. Therefore, the actual axial compressive ratio at the opening level is higher than that of the upper and lower levels. It can be observed from Figure 6(c) that the lateral load carrying capacity of the laminated walls with an opening increase with the increase of the axial ratio until the axial ratio reaches 0.3, and the increasing ratio of the lateral load carrying capacity gets smaller. The lateral load carrying capacity decreases substantially when the axial ratio is higher than 0.3, as is illustrated in Figure 6 (a) and Figure 7 (a). Therefore, higher axial ratio will induce more abrupt decrease of the load carrying capacity. It is indicated that if the axial ratio of the laminated walls with an opening is higher than the critical value (0.3), the risk of sudden failure of an element or a structure will be increased.

The deformation ductility ratio is defined as the ratio of the ultimate displacement to the yielding displacement. The deformation ductility is another important index to evaluate the seismic performance of an element. It can be found from Figures 6 that the force-displacement curves of the laminated walls with and without openings become more and more abrupt with the increasing of the vertical axial force, which is similar to the common cast-in-place RC walls. Generally speaking, the ductility decreases with the increase of the axial ratio as shown in Figure 7 (b).

Some of the tested and simulated results including the displacement ductility ratio are listed in Tables 4 to 6. Values in Tables 4 to 6 indicate that the tested results are consistent in each group, which can manifest the confidence of the test results. The average cracking displacement and yielding point of the top-displacement of the tested laminated walls are about 25% larger than those of the common cast-in-place RC walls. This indicates that the prefabricated part may delay the cracking and yielding under the axial ratio of 0.2. The lateral resistant capacity and the displacement ductility of the laminated walls are comparable to the conventional cast-in-place RC walls under this loading case. Therefore, the laminated wall has rather better load carrying and deformation capacity under this loading condition.

The lateral load carrying capacity is improved at first with the increase of the axial ratio and then decreased abruptly when the axial ratio exceeds a certain value as shown in table 5. And the deformation ductility ratio decreases with the increase of the axial ratio which can be found from this simulation results. High axial force decreases the deformation capacity of the laminated specimens, which is similar to the common cast-in-place RC walls.

The comparison between the simulation results of the cast-in-place wall (see Table 4) and the laminated walls (see Table 5) under different axial ratios indicates that the seismic performance

including load carrying and deformation capacity of laminated wall behaves well under low axial ratios. But the laminated wall becomes weaker to carry the lateral force and the lateral load carrying capacity decreases more abruptly compared with the common cast-in-place walls under high axial ratios especially the axial ratio is higher than the critical value.

The maximum lateral load of the laminated specimens with an opening varies from 677 kN to 793 kN (see Table 6), and the simulated maximum value is 518kN. The simulated result is lower than that of the test value by 31.7%. That may be due to the strengthening effect of the local strengthening steel bars of the connection beam and the local strengthening steel bars around the opening. The lateral load carrying capacity is enhanced with the increase of the axial ratio until the axial ratio reaches 0.3, and then decreases when the axial ratio is larger than 0.3. This pattern is similar to that of the solid laminated walls without openings and the common cast-in-place RC wall.

Table 4. Seismic behaviour of the common cast-in-place walls under different axial ratios

Specimen type	Specimen number	Axial ratio	Cracking load P_{cr} (kN)	Cracking displacement Δ_{cr} (mm)	Yield load P_y (kN)	Yield displacement Δ_y (mm)	Maximum load P_m (kN)	Ultimate load P_u (kN)	Ultimate displacement Δ_u (mm)	Displacement ductility μ
Tested specimen	SWA	0.20	600	4.04	738	7.5	1053	895	26.0	3.5
Simulated specimens	SWAC1	0.10	-	-	616	6.8	758	644	30.2	4.4
	SWAC2	0.15			731	7.7	890	756	26.6	3.5
	SWAC3	0.20	-	-	870	7.0	1026	873	23.0	3.3
	SWAC4	0.25			866	8.0	1030	875	21.5	2.7
	SWAC5	0.30	-	-	907	7.3	1046	904	23.0	3.2
	SWAC6	0.35			1040	8.2	1193	1014	18.2	2.2
	SWAC7	0.40	-	-	1068	8.2	1231	1046	17.0	2.1
	SWAC8	0.45			1095	8.0	1248	1060	15.6	2.0
	SWAC9	0.50	-	-	946	7.6	1085	922	22.8	3.0

*Note: Cracking load, Yield load and Ultimate load all refer to the lateral load. The yield point is determined using the method of the secant line of the 75% peak strength. The ultimate point is defined as the point when the lateral force decreases to 85% of the peak value or the specimen failure point on the force-displacement curve.

Table 5. Seismic behaviour of the solid laminated walls without openings under different axial ratios

Specimen type	Specimen number	Axial ratio	Cracking load P_{cr} (kN)	Cracking displacement Δ_{cr} (mm)	Yield load P_y (kN)	Yield displacement Δ_y (mm)	Maximum load P_m (kN)	Ultimate load P_u (kN)	Ultimate displacement Δ_u (mm)	Displacement ductility μ
Tested specimens	PCFA1	0.20	760	5.02	900	9.0	1012	860	32.4	3.6
	PCFA2	0.20	756	5.16	886	9.3	1045	888	30.0	3.2
	PCFA3	0.20	727	5.12	846	9.5	950	807	33.0	3.5
	PCFA4	0.20	693	5.32	803	9.6	915	778	31.0	3.2
Tested specimen	SWA	0.20	600	4.04	738	7.5	1053	895	26.0	3.5
Simulated specimens	PCFAC1	0.10	-	-	662	6.5	799	679	-	-
	PCFAC2	0.15			757	7.0	902	766	30.0	4.3
	PCFAC3	0.20	-	-	880	7.3	1017	864	25.7	3.5
	PCFAC4	0.25			933	7.4	1089	925	22.6	3.1
	PCFAC5	0.30	-	-	1015	7.7	1160	986	20.6	2.7
	PCFAC6	0.35			1047	7.8	1207	1021	18.6	2.4
	PCFAC7	0.40	-	-	995	7.5	1125	956	24.9	3.3
	PCFAC8	0.45			810	6.6	948	805	20.9	3.2
	PCFAC9	0.50	-	-	585	5.2	684	581	15.0	2.9

Comparing the force-displacement relationship of the common cast-in-place wall to the solid laminated wall, the laminated wall behaves more sensitive to the axial load. The maximum lateral carrying load of the common cast-in-place wall is 1248kN under the axial ratio of 0.45, and that of the solid laminated wall is 1207kN under the axial ratio of 0.35. The lateral carrying capacity of the laminated wall reaches its maximum value more quickly with the increase of the axial ratio. That is to say, the top drift is smaller when the lateral load reaches the maximum value. That can provide the evidence that the laminated wall is more sensitive with the variation of the axial ratio than the common cast-in-place RC wall.

From the above analysis on the lateral load carrying capacity and the deformation ductility of the three

kinds of walls under different axial ratios, it can be clear that the lateral load carrying capacity will increase firstly and then decrease with the increasing of the axial ratio, and the influence of the axial ratio on the laminated walls is more significant than the cast-in-place walls. The increasing of the axial ratio can weaken the deformation capability of the laminated walls, which is similar to the common cast-in-place walls. Here, the deformation ductility is defined as the ultimate deformation to the yield deformation. Because the definition of the yield value may be variable, the value of deformation ductility can only be considered as a reference index.

Table 6. Seismic behaviour of the laminated walls with an opening under different axial ratios

Specimen type	Specimen number	Axial ratio	Cracking load P_{cr} (kN)	Cracking displacement Δ_{cr} (mm)	Yield load P_y (kN)	Yield displacement Δ_y (mm)	Maximum load P_m (kN)	Ultimate load P_u (kN)	Ultimate displacement Δ_u (mm)	Displacement ductility μ
Tested specimens	PCFB1	0.10	459	5.0	623	10.9	793	589	29.9	2.7
	PCFB2	0.10	486	7.0	581	11.4	805	611	40.1	3.5
	PCFB3	0.10	477	6.7	586	11.4	755	532	32.0	2.8
	PCFB4	0.10	508	6.5	627	11.8	677	543	31.0	2.6
Simulated specimens	PCFBC1	0.10	-	-	424	3.5	518	440	-	-
	PCFBC2	0.15	-	-	500	4.2	567	482	32.0	7.6
	PCFBC3	0.20	-	-	558	4.3	613	521	21.4	5.0
	PCFBC4	0.25			541	3.2	650	553	13.2	4.1
	PCFBC5	0.30	-	-	567	3.2	663	563	11.0	3.4
	PCFBC6	0.35			532	2.8	650	553	8.9	3.2
	PCFBC7	0.40	-	-	533	2.9	623	529	7.0	2.4
	PCFBC8	0.45			461	2.3	573	487	5.6	2.4
	PCFBC9	0.50	-	-	422	2.3	465	395	3.8	1.7

4.3. Discuss of the Laminated Wall Integrity

Since the laminated RC wall is constructed with prefabricated plate and cast-in-place plate, the integrity of this kind of laminated wall should be discussed here. From above, the laminated wall behaved well on the integrity at the early stage of the test, but then there appeared vertical crack at the interface at the later stage of the test. The deformation of the prefabricated part and the cast-in-place part of the laminated walls matched up in general when they were in compression and the incompatible deformation behaved obvious when they were in tension. The vertical crack at the interface of the concrete with different ages emerged when the lateral load was close to the maximum value, and the horizontal cracks appeared almost simultaneously. After that, concrete of the laminated wall crushed at the corner and the crushing continued to the end of the test. The deformation incompatibility of the prefabricated part and the cast-in-place part was not so distinct even at the degradation stage of the nonlinear deformation developing procedure under this test condition.

The stress develop history of the simulation study shows that there is delay in stress development of the prefabricated part, and the vertical stress difference is more evident when the axial ratio is higher. That induces the quick decrease of the load carrying capacity. To sum up, the laminated walls with different concrete ages are not suggested to apply in high axial loading conditions, unless the integrity of the laminated wall is verified for the design loading cases.

5. CONCLUSIONS

The experimental and numerical simulation study of the laminated RC walls is presented in this paper. Two kinds of typical laminated walls with and without openings, and the common cast-in-place RC wall were tested under vertical and cyclical horizontal load. Numerical simulation was then carried out through the nonlinear analysis software ABAQUS. The analysis results were first verified with the tested results and the further simulation study was conducted on the specimens under different axial ratios. Based on the test and simulation results, the following conclusions can be drawn:

(a) The damage pattern, the lateral load carrying capacity and deformation characteristic of the partially prefabricated laminated walls are similar to the traditional cast-in-place RC walls.

(b) In the studied cases, the lateral load carrying capacity first increase and then decrease with the increase of the vertical load. The peak value of the lateral load carrying capacity appears at the axial ratio of 0.45, 0.35, and 0.3, for the common cast-in-place walls, solid laminated walls, and laminated walls with an opening, respectively.
(c) Axial ratio has important impact to the laminated walls. Similar to the common cast-in-place walls, the ductility of the laminated walls decreases with the increase of the axial ratio. But, the influence is more sensitive for the laminated walls than for the common cast-in-place walls.
(d) The incompatibility on the interface of precast and cast-in-place concrete can induce brittle failure when the axial ratio is higher than the critical value (0.35 for the solid laminated walls and 0.3 for the laminated walls with an opening in the studied cases).

The present laminated wall can be partly manufactured in factory, and the surface decoration and windows can be prefabricated. Therefore, the laminated wall is favourable for rapid construction, especially in the reconstruction in earthquake-hit areas. But, this kind of laminated wall is not suggested for application in high axial loading conditions, unless the integrity of the laminated wall is verified for the design loading cases.

ACKNOWLEDGEMENT

The financial support of National Natural Science Foundation of China (Grant No.: 51008226), Kwang-Hua Fund for College of Civil Engineering in Tongji University, The Research Fund for the Doctoral Program of Higher Education (Grant No.: 20090101120058), The Fundamental Research Funds of the Central Universities (2011QNA4016), is gratefully acknowledged. The staffs of State Key Laboratory of Disaster Reduction in Civil Engineering in Tongji University are also gratefully acknowledged.

REFERENCES

Dong, Y.G. and Lu, X.L. (2007). "Study on axial compression ratio calculation and limit value for steel reinforced concrete walls", *Journal of Earthquake Engineering and Engineering Vibration*, Vol. 27, No.1, pp. 80-85. (in Chinese)

Hallinan, P. and Guan, H. (2007). "Layered finite element analysis of one-way and two-way concrete walls with openings" *Advances in Structural Engineering*, Vol. 10, No. 1, pp. 55-72.

Huan Y., Fang Q., Chen L. and Zhang Y.D. (2008). "Evaluation of Blast-Resistant Performance Predicted by Damaged Plasticity Model for Concrete", *Transactions of Tianjin University*, Vol. 14, No.6, pp. 414-421. (in Chinese)

Kent D. C. and Park R. (1971) "Flexural members with confined concrete". *Journal of the Structural Division*, ASCE, Vol. 97, No. 7, pp. 1969-1990.

Li, H.H. and Li, B. (2006). "Study of a new macro-finite element model for seismic performance of RC shear walls using quasi-static experiments", *Advances in Structural Engineering*, Vol. 9, No. 2, pp. 173-184.

Ministry of Construction of the People's Republic of China. (2010). *Code for Design of Concrete Structures*, GB50010-2010, China Architecture & Building Press. Beijing. (in Chinese)

Saito, M., Yoshimatsu, T., Homma K, Saito, I. and Nakajima, R. (1995). "Trusses and precast concrete slabs reinforced thereby", U.S. Patent 5448866.

Salonikios, T.N., Kappos, A.J., Tegos, I.A. and Penelis, G.G. (1999). "Cyclic load behavior of low slenderness reinforced concrete walls: design basis and test results" *ACI Structure Journal*, Vol. 96, No. 4, pp. 649-660.

West, M. (2001). "Fabric-formed concrete structures" Proceedings of the First International Conference on Concrete and Development (C and D). Tehran, Iran. Apr 30-May 2, pp. 133-142.

Zhang, H.M., Lu, X.L. and Lu, L. (2007). "Influence of boundary element on seismic behavior of reinforced concrete shear walls", *Journal of Earthquake Engineering and Engineering Vibration*, Vol. 27, No. 1, pp. 92-99. (in Chinese)

Zhang, H.M., Lu, X.L., Li J.B. and Lu L. (2010a). "Cyclic load experiment study on the laminated laminated RC walls with different concrete ages", *Structural Engineering and Mechanics*, Vol. 36, No. 6, pp. 745-758.

Zhang, H.M., Lu, X.L. and Wu X.H. (2010b). "Experimental study and numerical simulation of the reinforced concrete walls with different stirrup in the boundary element". *Journal of Asian Architecture and Building Engineering*. Vol. 17, No. 2, pp. 447-454.